

# 3-D OBJECT RECONSTRUCTION FROM MULTIPLE-STATION PANORAMA IMAGERY

Thomas Luhmann, Werner Tecklenburg

University of Applied Sciences, Institute for Applied Photogrammetry and Geoinformatics,  
Ofener Str. 16, D-26121 Oldenburg, Germany – (luhmann, tecklenburg)@fh-oldenburg.de

Commission V, WG V/1

**KEY WORDS:** Panorama, panoramic imagery, 3-D, multi-image, epipolar lines, space intersection

## ABSTRACT:

The paper discusses the potential of photogrammetric multi-station panorama processing for the 3-D reconstruction of objects. We cover the complete process from image acquisition, panorama generation by frame imagery and by rotating line-scanner imagery, calibration, tie point and control point measurement, panorama bundle adjustment to the final image compilation of 3-D objects.

The IAPG owns several high-resolution digital cameras, e.g. Kodak DCS 460, Fuji FinePix S1 Pro and S2 Pro, Sigma SD 10 and Kodak/Mamiya DCS 645M. These devices can be used for panorama image acquisition if a suitable camera mount is used. In this case single image frames can easily be stitched together to a complete or partial panorama under consideration of the strict camera model (calibration parameters). Alternatively, our rotating line-scanner camera KST EyeScan can be used that produces very high resolution images. Both approaches have advantages and disadvantages that have been discussed in previous papers.

If at least three different panoramas have been generated from different local stations, they can be oriented by bundle adjustment. Due to the stable geometry of the cylindrical panorama model the bundle adjustment can be performed with very few object points. Once each panorama is oriented with respect to global coordinate system, photogrammetric object reconstruction procedures such as space intersection or a moving floating mark can be applied.

Two practical examples demonstrate the process of panorama object recording and modeling. The entrance hall of the university has been reconstructed in 3-D yielding a wireframe model of the interior. For the Great Hall of the Oldenburg castle again four panoramas have been processed whereby special effort has been spent to produce a high-quality color panorama.

## 1 INTRODUCTION

Panorama imagery is becoming more and more popular for 360° presentations of natural environments, e.g. for touristic purposes (e.g. [www.oldenburg.de](http://www.oldenburg.de)), metric site documentation for facility management applications (Chapman & Kotowski, 2000), or for the combination with 3-D laser-scanners. Panoramic images are mostly created by off-the-shelf stitching programs (e.g. Photovista Panorama) that can match uncalibrated frame images into a cylindrical projection with limited user interactions. A closer view to the resulting image quality of such programs shows that image deformations occur if lens distortion is not considered properly (Luhmann & Tecklenburg, 2002, 2003).

The recent generation of digital rotating line scanners offers very high geometric and radiometric resolution (Scheele et al., 2001). A special problem is rising since the geometric quality of such a camera is mainly depending on the mechanical precision of the scanning device, and the concentricity between perspective centre and rotating axis. In most cases it is assumed that pre-calibrated camera parameters remain constant for a longer period in time. Remaining calibration errors lead to a non-linear deformation of the cylindrical image that can only be handled if on-the-job camera calibration by bundle adjustment is performed.

Panoramic images from multiple stations can be used for the 3-D reconstruction of objects. Due to the cylindrical constraints of panoramas the orientation of multiple panoramic images can be calculated with much less tie points than for usual image bundles. It has been shown that only 5-7 tie points in 3-D space are necessary to compute a bundle adjustment for a number of >3 single panoramic images (Luhmann & Tecklenburg, 2002). Similar approaches have been used to model archaeological

environments (Petsa et al, 2001). The concept of two frame cameras mounted on a rotating bar has been discussed by (Heikkinen, 2002) where the advantage of cylindrical constraints is combined with stereo capability for 3-D reconstruction.

## 2 PANORAMA IMAGE ACQUISITION

### 2.1 Frame imagery

In order to create panorama images for photogrammetric object reconstruction, modern digital cameras can be used. If high precision and resolution shall be achieved, professional digital cameras can be applied that offer up to 4000 x 4000 pixels or even more (Peipe 2004).

As described in Luhmann & Tecklenburg (2003) digital frame cameras yield high quality panoramic images if the whole imaging and resampling process is performed under strict consideration of geometric properties of all involved components. The two most critical features refer to the calibration of the camera, and the adjustment of the rotating panorama adapter with respect to the (calibrated) principal point.

The panorama generation can be summarized as follows:

1. Camera calibration (for non-metric cameras)
2. Adjustment of panorama adapter (principal point lies on rotation axis)
3. Image acquisition (number of images depend on focal length, appropriate image overlap required)
4. Measurement of tie points (automation possible by interest operators or feature matching)

5. Bundle orientation of image set (result are orientation parameters of each single image)
6. Panorama resampling (a cylindrical panorama images is resampled from the original images with adjustable resolution)



Fig. 1: Digital camera Kodak DCS 645M mounted on panorama adapter

Although the above mentioned process seems to require a high amount of work, most of the steps can be handled easily or they can be automated. Since there is no stitching process where overlapping image areas are analyzed and "pasted" together, the presented approach leads to accurate panoramas where the border between two source images is almost not visible. However, if invalid camera calibration parameters exist, or if the panorama adapter adjustment is insufficient, displacement errors remain in the final panoramic image.

## 2.2 Rotating line scanner

The process of panoramic image acquisition becomes more convenient if a rotating line scanner is used as shown in Fig. 2.



Fig. 2: Digital panorama line-scanning camera KST EyeScan M3

The digital panoramic line-scanning camera KST EyeScan M3 (Fig. 2) has been developed in collaboration between KST and DLR (Scheele et al., 2001). It offers superb images of highest geometric and radiometric resolution (see Fig. 3 and Fig. 4). It consists of an 10200 pixel RGB CCD line sensor with infrared filter. Lenses of 35mm and other focal lengths are available. Depending on the lens full panoramic images consist of up to 54000 columns leading to a maximum image size of 1.8 GB.



Fig. 3: Panoramic image generated by EyeScan M3, 35mm lens (IAPG building)



Fig. 4: Original image window from Fig. 3 (see arrow and square)

The geometric accuracy of the camera has been investigated by Schneider & Maas (2003, 2004). A sophisticated set of parameters has been found that handles most of the geometric and mechanical errors of the camera.

## 3 3-D RECONSTRUCTION

### 3.1 Collinearity equations

In order to derive the collinearity equations for cylindrical panorama images, an object point  $(X, Y, Z)$  is transformed into a local Cartesian coordinate system by the exterior orientation parameters of panorama cylinder (compare Schneider & Maas 2003).

$$\begin{bmatrix} X_{Cyl} \\ Y_{Cyl} \\ Z_{Cyl} \end{bmatrix} = \begin{bmatrix} r_{11} \cdot (X - X_o) + r_{21} \cdot (Y - Y_o) + r_{31} \cdot (Z - Z_o) \\ r_{12} \cdot (X - X_o) + r_{22} \cdot (Y - Y_o) + r_{32} \cdot (Z - Z_o) \\ r_{13} \cdot (X - X_o) + r_{23} \cdot (Y - Y_o) + r_{33} \cdot (Z - Z_o) \end{bmatrix} \quad (1)$$

Using the scaling factor

$$\lambda = \frac{r}{\sqrt{X_{Cyl}^2 + Y_{Cyl}^2}} \quad (2)$$

the relationship between object coordinates and pixel coordinates of the panorama image yields

$$x'_{pix} = r \cdot \arctan\left(\frac{X_{Cyl}}{Y_{Cyl}}\right) + \Delta x \quad (3)$$

$$y'_{pix} = y_h - Z_{Cyl} \cdot \lambda + \Delta y$$

where  $\Delta x, \Delta y$  are corrections given by camera calibration functions, and  $y_h$  a vertical shift due to a tilted image horizon.

### 3.2 Epipolar geometry

For large panorama images the determination of homologous points can be difficult since the visual impression is, in the first instance, unusual, and large bitmaps are not easy to handle. If epipolar lines are available, the search space for homologous object features can be restricted significantly.

The epipolar plane is defined as the plane built by an object point P and the two image points P', P'', or the two principal points O', O'', respectively. The epipolar plane intersects the panorama cylinder in an arbitrary position and orientation, hence an ellipse is resulting as intersecting curve (Fig. 5). In contrast to perspective images panoramic epipolar lines appear as sine curves in the panorama image matrix.

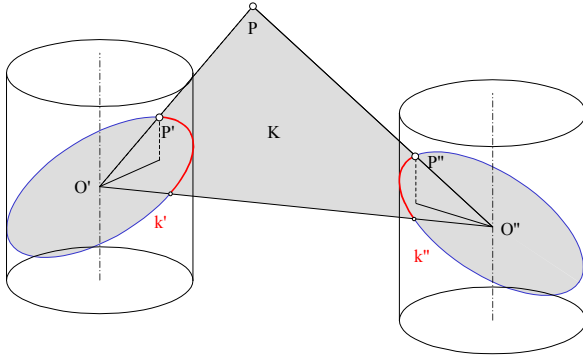


Fig. 5: Epipolar plane K and epipolar lines k' and k''

The sine form of the epipolar lines can easily be proven. For a measured point P' an arbitrary object point P on the image ray of P' can be calculated. The corresponding image coordinates  $x'', y''$  in the second panorama can be calculated according to eq. (3). If the epipolar plane intersects the panorama cylinder under an angle  $\beta$  or the slope  $m = \tan \beta$ , the intersecting line builds a straight line of  $z' = m \cdot x'$  according to Fig. 6. Hence, with

$$z' = m \cdot r \cdot \sin \alpha \quad (4)$$

a sine function is obtained.

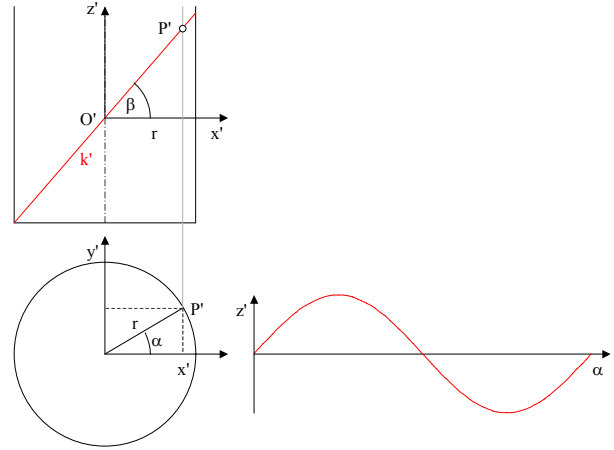


Fig. 6: Sinusoidal form of panoramic epipolar lines

### 3.3 Bundle adjustment

Based on the collinearity equations (3) the bundle adjustment program for panoramic imagery PANO has been developed. Compared to central-projective imagery the major benefit of panorama bundles is the possibility to have image observation over the complete horizon (Fig. 7). This leads to a minimized effort in image point measurement, especially for interactive measurements which form the most common task in applications like as-built documentation or indoor reconstructions.

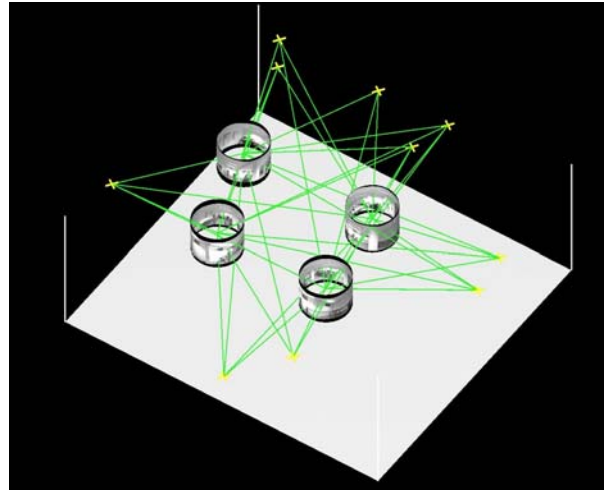


Fig. 7: Distribution of 4 panoramas in 3-D space

With four given panoramas it is, in theory, possible to perform a bundle triangulation with a minimum of four object points. Assuming a free-net adjustment, a total of  $4 \cdot 6 = 24$  unknown orientation parameters plus  $4 \cdot 3 = 12$  unknown 3-D coordinates minus 7 datum parameters have to be determined. The resulting 29 unknowns can be solved by 32 observation equations (4 panoramas \* 4 object points \* 2 equations), hence a redundancy of 3 is obtained. The system can be solved if the object points do not lie on a common straight line. However, the equation system is extremely sensitive against gross errors, as demonstrated in the following example (Fig. 8).

	4 tie points	8 tie points	16 tie points
X	421,6mm	8,9mm	1,7mm
Y	357,1mm	8,5mm	1,6mm
Z	76,8mm	2,9mm	1,2mm

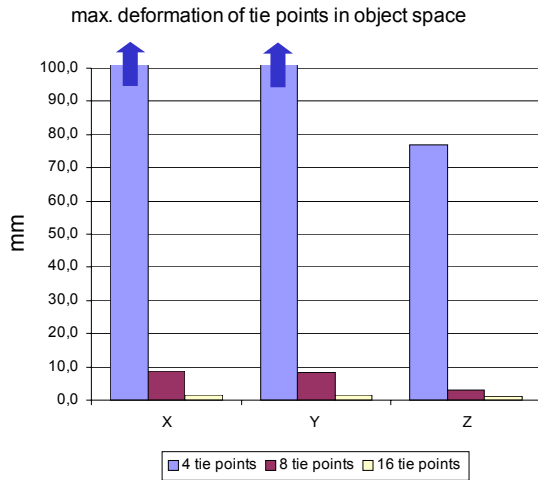


Fig. 8: Effect of one gross error to different number of tie points

If one image coordinate of a tie point is manipulated by a gross deviation of 5 pixels, the system becomes unstable for the minimum number of 4 tie points. If 8 well-distributed tie points are used (Fig. 9), the system becomes significantly more reliable. In this case, 32 additional equations are obtained with only 12 additional unknowns. With a resulting total redundancy of 23 (instead of 3) gross errors can easily be detected. A further increase to 16 tie points yields to even better results.



Fig. 9: Distribution of 8 tie points

Consequently, for practical applications with a small number of tie points, residuals should be analyzed, and tie points must be controlled. However, the effort of additional point measurement is fairly small.

### 3.4 Space intersection

After bundle adjustment exterior orientation parameters are available for each panorama. Subsequently, additional homologous image points can be measured yielding 3-D object coordinates by space intersection. The observation equations for panoramic space intersection are either based on the panoramic collinearity equations (3), or the standard collinearity equations for central-projective imagery can be applied. In the latter case, the measured panorama pixel coordinates must be transformed into Cartesian cylinder image coordinates as follows:

$$\begin{aligned}
 x' &= r \cdot \sin \alpha \\
 y' &= r \cdot \cos \alpha \\
 z' &= y'_{Pix}
 \end{aligned}
 \quad \text{with } \alpha = \frac{x'_{Pix}}{r}
 \quad (5)$$

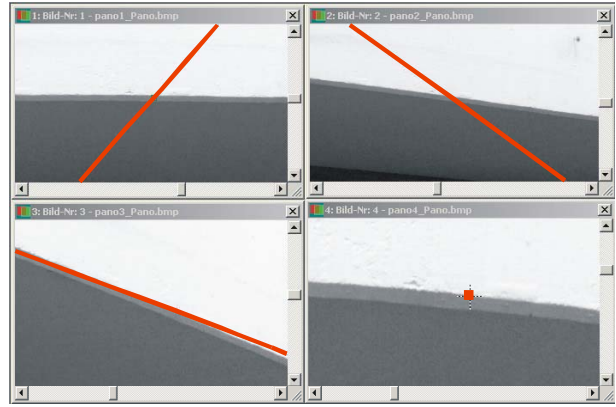


Fig. 10: Epipolar lines in 4 panoramas (lines graphically enhanced)



Fig. 11: Epipolar lines superimposed to an overview image

Using epipolar lines is a useful method if object points shall be measured that hardly can be identified (e.g. points on arcs in Fig. 9, or on an edge in Fig. 10). If an object point lies on a linear feature (e.g. an edge) that is part of the epipolar plane, the epipolar line does not intersect the feature in image space (Fig. 10, lower left). For multiple-station panoramas there is at least one epipolar line that intersects the image edge uniquely, as shown in the upper images of Fig. 10.

However, in contrast to standard photogrammetry, multiple-station panoramas may lead to a special situation. Since panorama images are usually acquired by cameras mounted on a tripod (regardless of frame or line-scanner imagery), their exterior orientation parameters have similar  $Z_0$  values. Object points with  $Z \approx Z_0$  lead to horizontal epipolar lines that can not be used for the measurement of horizontal object features.

As a consequence, at least 4 panoramas should be acquired whereby 2 of them should be shifted in Z direction according to Fig. 12.

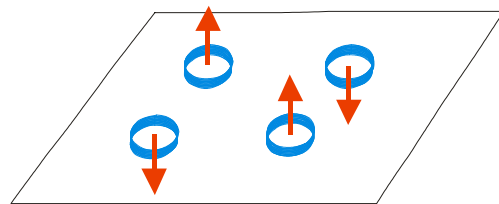


Fig. 12: Recommended shift in Z for panorama camera position

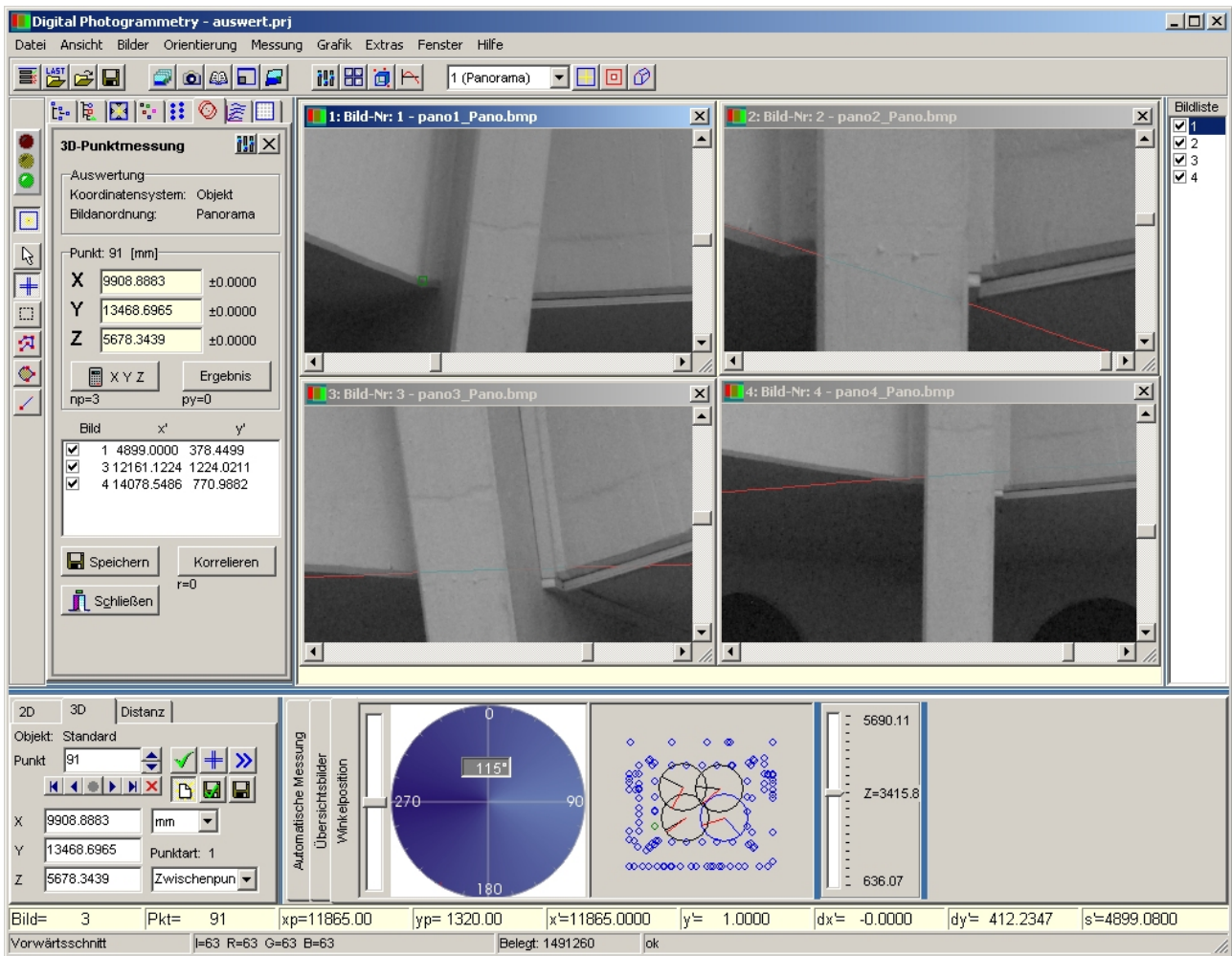


Fig. 13: User-interface of StereoMess

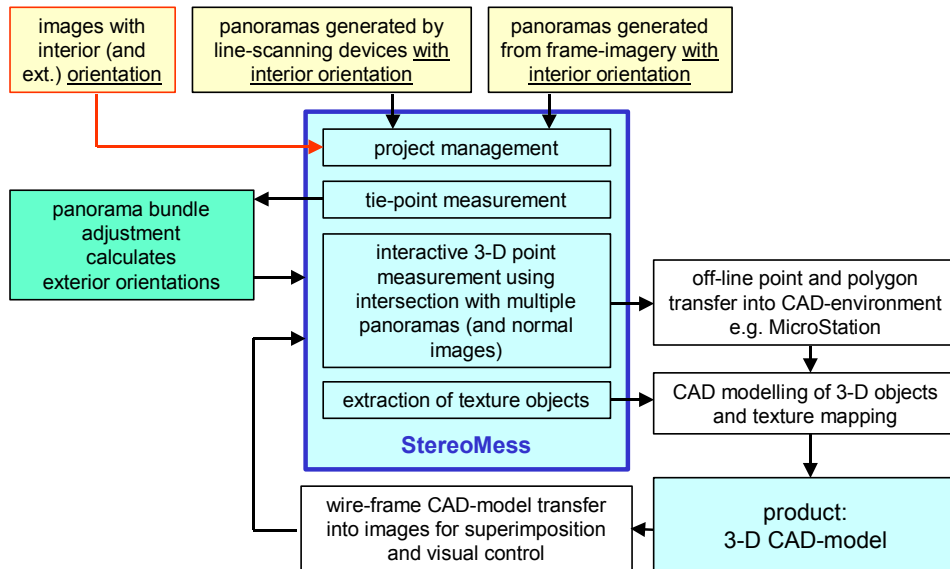


Fig. 14: Work-flow for 3-D object reconstruction from panoramic imagery

## 4 PRACTICAL EXAMPLES

### 4.1 Software package StereoMess

Photogrammetric object reconstruction is performed by the program StereoMess, a powerful interactive learning tool for students (Fig. 13). Beneath other features, StereoMess provides full panorama image modeling, epipolar geometry, image rectification, multiple image processing and much more.

The interactive evaluation of large panorama images taken from multiple stations require an ergonomic way of image handling, data representation and graphical tools. For this purpose StereoMess provides tools for object point selection and image scrolling as displayed in Fig. 15. The oriented panoramas are drawn in the XY plane whereby the angular zero position of each panorama image is displayed, and the direction to a selected object point is outlined. Using the track bar on the right a mean Z value can be selected. When the operator moves the mouse through the navigation window every image is panned and scrolled to the corresponding object position.

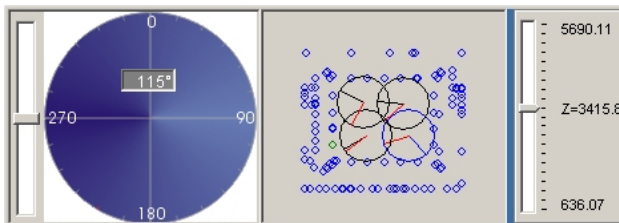


Fig. 15: Panorama image navigation

For 3-D object reconstruction two different approaches may be suitable: Firstly, panorama images can be rectified to object planes where digitizing or mono-plotting of object features can be performed (orthophoto examples in Fig. 16).

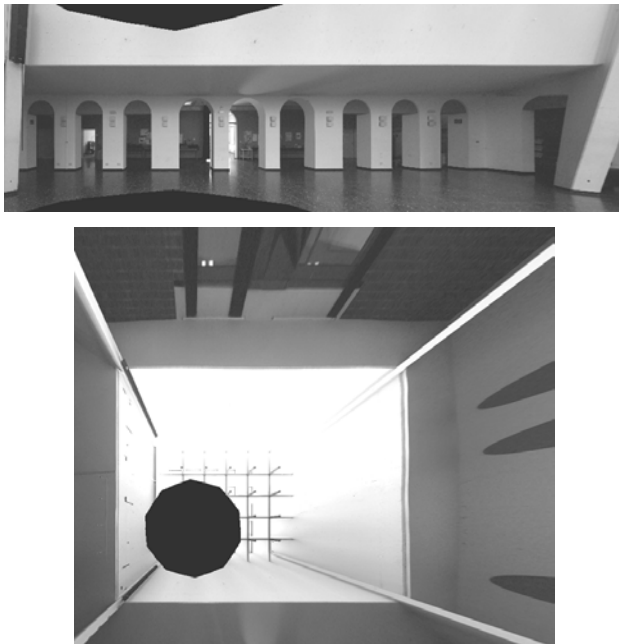


Fig. 16: Orthophotos generated from panorama imagery

Alternatively, a true 3-D measurement can be carried out based on space intersection of object points. Fig. 14 displays the

principle work-flow for 3-D object reconstruction. The system can process standard photogrammetric images and panoramic images simultaneously, i.e. images from arbitrary sources can be mixed within one project. StereoMess allows for the measurement of discrete points that can be topologically combined to 3-D polygons. 3-D object data can be exported to a CAD system via DXF where additional editing can be performed. The reverse data transfer from CAD to StereoMess has not been implemented yet.

### 4.2 Entrance hall

The first example deals with the 3-D reconstruction of the entrance hall of the University of Applied Sciences in Oldenburg. The dimensions of the hall are about 25m x 25m x 8m. It consists of a number of arcs that form the arcades on three sides of the hall. Four panorama images have been generated based on high-resolution frame imagery (Kodak DCS 645M). The mean pixel size in object space results to about 2mm.

For this example, 170 object points have been measured in order to provide basic geometry data for the 3-D reconstruction. The average accuracy of object points measured by space intersection is estimated to about 5mm depending on geometrical intersection conditions. This result corresponds to an image accuracy of about 2 pixel. A higher accuracy of about 1 pixel can be expected if better calibration parameters of the Kodak camera were available. In this case, the camera has been calibrated a couple of days before the actual measurement.

For the final 3-D model repeatedly occurring object features have been added by copying object elements within the CAD system (Fig. 17).

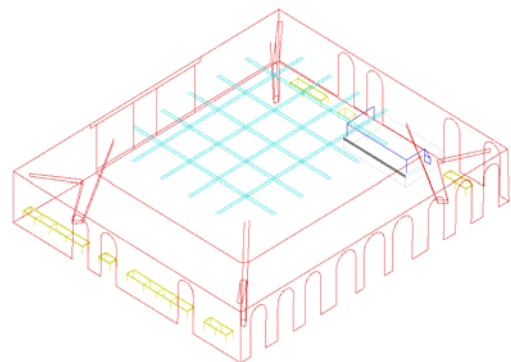


Fig. 17: 3-D model of the entrance hall

### 4.3 Great Hall, Oldenburg castle

The Great Hall of the Oldenburg castle has been surveyed within a student's project. Again, the Kodak DCS 645M camera was used to acquire four panoramas located in close to the four corners of the hall (Fig. 20). One additional panorama has been taken from the center of the hall in order to provide image data for a high-quality panorama presentation of the interior. A number of control points has been measured by non-contact tachymetry.

Each panorama originally consists of 10 frame images (Fig. 18). Based on calibrated camera data and a number of tie points measured in the overlapping zones of each image, the complete

panoramas could be resampled (Fig. 19). The final panorama image has a resolution of about 25900 x 5300 pixels.



Fig. 18: Original images of one panorama station

## 5 SUMMARY

The paper has discussed the potential of 3-D object reconstruction from multiple-station panoramic images. Based on geometrically calibrated panoramas that may be generated by

frame imagery or by rotating line scanners, collinearity equations for panoramic images can be derived. They can be applied to standard photogrammetric procedures such as bundle adjustment, space intersection or epipolar geometry.

The routines have been implemented into the interactive photogrammetric program StereoMess that enables 3-D multi-image processing for standard frame images, and panoramas as well. Two practical examples of indoor room reconstruction show the usage of panorama imagery for 3-D reconstruction.

The major benefit of multiple-station panoramas is the measurement of interiors since with only 3 stations (4 are recommended) and very few tie and control points, a complete 3-D model of the interior of a room can easily be achieved. In contrast, standard multi-image photogrammetry requires a high number of images where often weak ray intersection conditions occur.

## REFERENCES

Chapman, D., Kotowski, R., 2000: Methodology for the Construction of Large Image Archives of Complex Industrial Structures. *Publikationen der DGPF*, Band 8, Essen 1999.

Heikkinen, J. (2002): Performance of circular image blocks in close-range photogrammetry. *ISPRS Symposium Comm. V*, Korfu, 2002.

Luhmann, T. (ed.), 2001–2004: *Optische 3D-Messtechnik, Photogrammetrie, Laserscanning. Beiträge der Oldenburger 3D-Tage*, Wichmann Verlag, Heidelberg.

Luhmann, T., Tecklenburg, W. (2002): Bundle orientation and 3-D object reconstruction from multiple-station panoramic imagery. *ISPRS Symposium Comm. V*, Korfu, 2002.

Luhmann, T., Tecklenburg, W., 2003: Potential of panoramic views generated from high-resolution frame images and rotating line scanner images. Grün/Kahmen (eds.): *Optical 3-D Measurement Techniques*, ETH Zürich, pp.114-121.

Peipe, J. (2004): Wieviele Pixel braucht der Mensch? Luhmann (ed.): "Photogrammetrie – Laserscanning - Optische 3D-Messtechnik", Wichmann Verlag, 2004 (in press).

Petsa, E., Kouroupis, S., Karras, G.E. (2001): Inserting the past in video sequences. *International Archives of Photogrammetry, Remote Sensing and Spatial Information Systems*, Vol. XXXIV-5C7, pp. 707-712.

Scheele, M., Börner, A., Reulke, R., Scheibe, K. (2001): Geometrische Korrekturen: Vom Flugzeugscanner zur Nahbereichskamera. *Photogrammetrie-Fernerkundung-Geoinformation*, Heft 1, 2001, pp. 13-22.

Schneider, D., Maas, H.-G. (2003): Geometrische Modellierung und Kalibrierung einer hochauflösenden digitalen Rotationszeilenkamera. Luhmann (ed.): "Photogrammetrie – Laserscanning - Optische 3D-Messtechnik", Wichmann Verlag, 2003.

Schneider, D., Maas, H.-G. (2004): Einsatzmöglichkeiten und Genauigkeitspotential eines strengen mathematischen Modells für Rotationszeilenkameras. Luhmann (ed.): "Photogrammetrie – Laserscanning - Optische 3D-Messtechnik", Wichmann Verlag, 2004 (in press).



Fig. 19: Resulting panorama of Great Hall (camera station in hall center)

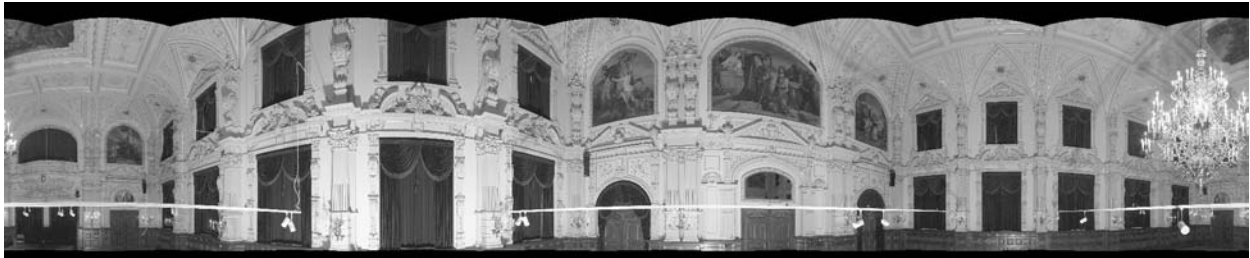


Fig. 20: Four measurement panoramas (cameras stations in hall corners)